www.nature.com/aps

Acta Pharmacologica Sinica

ARTICLE

MicroRNA-302a promotes neointimal formation following carotid artery injury in mice by targeting PHLPP2 thus increasing Akt signaling

Ying-ying Liu[1], Xiu Liu[1], Jia-guo Zhou[1] and Si-jia Liang[1]

The excessive proliferation and migration of smooth muscle cells (SMCs) play an important role in restenosis following percutaneous coronary interventions. MicroRNAs are able to target various genes and involved in the regulation of diverse cellular processes including cell growth and proliferation. In this study we investigated whether and how MicroRNAs regulated vascular SMC proliferation and vascular remodeling following carotid artery injury in mice. We showed that carotid artery injury-induced neointimal formation was remarkably ameliorated in microRNA (miR)-302 heterozygous mice and SMC-specific miR-302 knockout mice. In contrast, delivery of miR-302a adenovirus to the injured carotid artery enhanced neointimal formation. Upregulation of miR-302a enhanced the proliferation and migration of mouse aorta SMC (MASMC) in vitro by promoting cell cycle transition, whereas miR-302a inhibition caused the opposite results. Moreover, miR-302a promoted Akt activation by corporately decreasing Akt expression and increasing Akt phosphorylation in MASMCs. Application of the Akt inhibitor GSK690693 (5 μmol/L) counteracted the functions of miR-302a in promoting MASMC proliferation and migration. We further revealed that miR-302a directly targeted at the 3′ untranslated region of PH domain and leucine rich repeat protein phosphatase 2 (PHLPP2) and negatively regulated PHLPP2 expression. Restoration of PHLPP2 abrogated the effects of miR-302a on Akt activation and MASMC motility. Furthermore, knockdown of PHLPP2 largely abolished the inhibition of neointimal formation that was observed in miR-302 heterozygous mice. Our data demonstrate that miR-302a exacerbates SMC proliferation and restenosis through increasing Akt signaling by targeting PHLPP2.

Keywords: microRNA-302a; neointimal formation; vascular smooth muscle cell; proliferation; Akt; PHLPP2

Acta Pharmacologica Sinica (2021) 42:550–559; https://doi.org/10.1038/s41401-020-0440-4

INTRODUCTION

Vessel narrowing can contribute to various vascular diseases, such as stroke, hypertension, and heart attack [1]. Percutaneous coronary interventions (e.g., balloon angioplasty or stenting) are considered the first-choice treatment for acute coronary syndromes [2]. Unfortunately, patients face an increased risk of restenosis after surgery, leading to repeated interventions and a substantial economic burden [3]. Even though the application of bare-metal stents decreases the risk of restenosis to 20%–30% [3], the outcomes seem to still be unsatisfactory. Excessive smooth muscle cell (SMC) proliferation, migration and invasion are considered important contributors to restenosis, which together lead to neointimal hyperplasia [4, 5]. Therefore, inhibition of SMC hyperplasia is an important therapeutic approach for restenosis.

MicroRNAs (miRNAs) are a family of endogenous noncoding small RNAs consisting of 18–22 nucleotides that can regulate gene expression at the posttranscriptional level by pairing with imperfect complementary target sites in the 3′ untranslated region (3′UTR) of their target mRNAs [6, 7]. MiR-302 was initially identified in human embryonic stem cells and is critical for embryonic development, since mice deficient for miR-302 have a fully penetrant late embryonic lethal phenotype [8–10]. MiR-302a belongs to the miR-302 family, which includes miR-302a, miR-302b, miR-302c, miR-302d, and miR-367 [9]. These miRNAs are encoded by the miR-302–367 cluster located in the 4q25 locus of human chromosome 4 [9]. Previous studies have suggested that in addition to regulating embryonic development, miR-302a functions as a tumor suppressor by inhibiting Akt-dependent cell proliferation in different cancer cells, indicating that miR-302a may negatively regulate Akt activation [11–13]. Moreover, in a study by Li and colleagues, miR-302a affected Akt activation in neurons by silencing phosphate and tension homology (PTEN) [14]. Given the importance of Akt in regulating cell proliferation [5, 15], we speculated that miR-302a is involved in Akt-mediated vascular SMC (VSMC) proliferation and restenosis. In the present study, we demonstrate that miR-302a accelerates VSMC proliferation and subsequent neointimal formation by activating Akt signaling.

MATERIALS AND METHODS

MiR-302 heterozygous mice

MiR-302 heterozygous mice (miR-302$^{+/-}$) were generated on the C57BL/6 background at Nanjing Model Animal Research Center

[1]Department of Pharmacology, and Cardiac & Cerebral Vascular Research Center, Zhongshan School of Medicine, Sun Yat-Sen University, Guangzhou 510080, China
Correspondence: Si-jia Liang (liangsj5@mail.sysu.edu.cn)

Received: 5 January 2020 Accepted: 12 May 2020
Published online: 21 July 2020

using the CRISPR/Cas9 gene targeting method. Linearized Cas9-encoding vector and sgRNA mRNA were microinjected into the cytoplasm of thezygote, which was transferred into the oviductal ampullae of female mice. The genotyping of mice was performed by PCR on tail DNA using specific primers (Fig. S1a and Table S1).

MiR-302 conditional knockout mice

Mice with SMC-specific deletion of miR-302 (miR-302^{SMCKO}) were established using Cre/loxP recombination. The miR-302$^{flox/flox}$ allele was generated by flanking the 5 miRNAs (miR-302a, miR-302b, miR-302c, miR-302d, and miR-367) in this cluster with loxP sites in embryonic stem cells. SM22α-Cre transgenic mice were obtained from the Jackson Laboratory (Bar Harbor, ME) and then backcrossed to a C57BL/6 genetic background for at least nine generations. The genotyping strategy is shown in Fig. S2a, b, and the primers are listed in Table S1. All animal procedures were performed in accordance with the Institutional Animal Care and Use Committee at Sun Yat-Sen University.

Carotid artery injury model

For all surgical procedures, 8-week-old male mice were anesthetized by intraperitoneal injection with pentobarbital sodium (50 mg/kg). Surgery was carried out using a dissecting microscope (SMZ-800, Nikon, Tokyo, Japan). A guide wire (0.38 mm in diameter) was inserted into the left common carotid artery and slid 3 times. The miR-302a adenovirus (Ad-miR-302a) was generated by cloning the stem-loop sequence of mmu-miR-302a into the pAdTrack-CMV viral shuttle vector. Ad-lacZ was used as a negative control. Recombinant adenovirus harboring leucine rich repeat protein phosphatase 2 (PHLPP2) shRNA (Ad-shPHLPP2) was synthesized by Ubigene (Guangzhou, China). The adenovirus (1.0×10^{11} PFU) was delivered to the injured artery and incubated for 30 min. The carotid arteries were collected for various times as indicated.

Quantitative real-time PCR (qRT-PCR)

Two micrograms of RNA isolated from mouse aorta SMCs (MASMCs) using TRIzol reagent were reverse-transcribed with a PrimeScript RT reagent kit (Bio-Rad Laboratories, Hercules, CA) as previously described [16, 17]. Real-time PCR was amplified on a MyiQ Single Color Real-time PCR Detection System (Bio-Rad Laboratories) using SYBR Green PCR Master Mix (Invitrogen, Carlsbad, CA). To detect miRNA expression, reverse transcription was performed using the TaqMan® MicroRNA Reverse Transcription Kit (Applied Biosystems, Carlsbad, CA), and PCRs were conducted using the TaqMan® MicroRNA Assay Kit (Applied Biosystems). The sequence-specific primers were as follows: PHLPP2 forward: 5′-GGGAGCACTTGGCTGTTACT-3′, reverse: 5′-GGGAGTACTTGCCCAACCTC-3′; 18S rRNA forward: 5′-GCAATTAT TCCCCATGAACG-3′, reverse: 5′-GGCCTCACTAAACCATCCAA-3′; miR-302a forward: 5′-AATAAGTGCTTCCATGTTTTGGTGA-3′; and U6 forward:5′-ATTGGAACGATACAGAG-3′, reverse: 5′-GGAACGCTT-CACGAATTTG-3′. The fold change in gene expression was calculated using the $2^{-\Delta\Delta CT}$ method, with 18S rRNA or U6 as an internal control.

Morphometry

After euthanasia, the injured segment of the common carotid artery was dissected from the surrounding tissue, fixed in 10% formalin, dehydrated in 30% sucrose solution each for 24 h, and finally embedded longitudinally in OCT. Samples were cut into 8-μm longitudinal sections to assess intimal lesion size by hematoxylin-eosin (HE) staining. The external plastic layer (EPL) area, the internal plastic layer (IPL) area, and the luminal area were measured with ImageJ (version 1.44, NIH, Bethesda, MD). The intimal/medial ratio was calculated as follows: Intimal thickness = $(\text{IPL area}/\pi)^{1/2}$-$(\text{luminal area}/\pi)^{1/2}$; medial thickness = $(\text{EPL area}/\pi)^{1/2}$-$(\text{IPL area}/\pi)^{1/2}$.

Western blotting analysis

Western blotting was performed as described previously [7, 16, 17]. Protein was extracted from MASMCs using protein lysis buffer (Beyotime, Shanghai, China) and separated using 10% SDS-PAGE gels. Primary antibodies against the following antigens were used: Akt (#4691S), p-Akt (Ser473) (#4060S), cyclin E1 (#20808), CDK2 (#2546), p27(#3686S), PTEN (#9188 S), PDK1 (#5662S), MMP9 (#13667S), MMP2 (#40994S), p85 (#4228S), p110 (#5405S), β-actin (#3700S), GAPDH (#5174S) (Cell Signaling Technology, Danvers, MA); PCNA (ab29), PHLPP2 (ab71973) (Abcam, Cambridge, MA); and p21(05-345) (Millipore, Billerica, MA). After incubation with horseradish peroxidase (HRP)-linked anti-mouse IgG (#7076) or HRP-linked anti-rabbit IgG (#7074) (Cell Signaling Technology) for 1 h, blots were visualized with an ECL kit and quantified with ImageJ software.

Immunohistochemistry

The sections of carotid arteries were treated with 3% H_2O_2 in phosphate-buffered saline (PBS) for 10 min to inhibit intrinsic peroxidase activity and then incubated with 5% blocking solution for 1 h to prevent nonspecific antibody binding. Antigen retrieval for cross sections was performed with citrate buffer (pH 6.0). The sections were incubated with an antibody against Ki67 (ab15580, Abcam) overnight at 4 °C. After rinsing in PBS, sections were incubated with anti-rabbit IgG for 20 min at room temperature, followed by DAB and hematoxylin staining.

Cell culture and treatment

Primary MASMCs were isolated from the aortas of male C57BL/6 mice (4–6 weeks) as described previously [5]. Briefly, the mice were deeply anesthetized with intraperitoneal injection of pentobarbital sodium. The aortas were cut up with scissors and then cultured in 5 mL Dulbecco's modified Eagle's medium (DMEM) containing 10% fetal bovine serum (FBS) and 1% penicillin-streptomycin (Gibco, Waltham, MA). Cultures were maintained at 37 °C in a humidified incubator in a 95% O_2 plus 5% CO_2 atmosphere.

Cell transfection

MiR-302a mimics, mimics negative control, miR-302a inhibitor, inhibitor negative control, PTEN siRNA, and scramble RNA were obtained from GenePharma (Shanghai, China). PTEN and PHLPP2 plasmids were constructed with a full-length cDNA fragment of the mouse PTEN gene and PHLPP2 gene, respectively, which were PCR-amplified from MASMC RNA and then cloned into the pCMV vector using *EcoR*I and *BamH*I restriction enzymes. All of the reagents were transfected into MASMCs using Hiperfect transfection reagent (Qiagen, Valencia, CA) according to the manufacturer's instructions.

Cell viability assay

Cell viability was measured by the Cell Counting Kit-8 (CCK-8, Dojindo Molecular Technologies, Rockville, MD) assay. MASMCs were cultured in 96-well culture plates (1×10^5 cells/well) and transfected with miR-302a mimics, miR-302a inhibitor, or their corresponding controls for 24 h. Afterwards, cells were treated with or without 20 ng/mL recombinant mouse platelet-derived growth factor-BB (PDGF-BB) (Sigma, St. Louis, MO) for 24 h or cultured in DMEM supplemented with or without 10% FBS for 24 h. CCK-8 solution (10 μL) was added to each well for another 2 h. The absorbance was detected at 450 nm by a microplate reader (Bio-Tek, Winooski, VT).

BrdU incorporation

MASMC proliferation was measured based on the incorporation of BrdU as previously described [5]. Cells were treated with 10 mmol/L BrdU (Sigma) for 4 h prior to incubation with BrdU antibody (B2531) (Sigma) for 1 h at room temperature. Afterwards, the cells were treated with HRP-linked anti-mouse IgG for 1 h. Then, 100 μL of 3,3′,5,5′-tetramethylbenzidine (100 mmol/L) was added as the

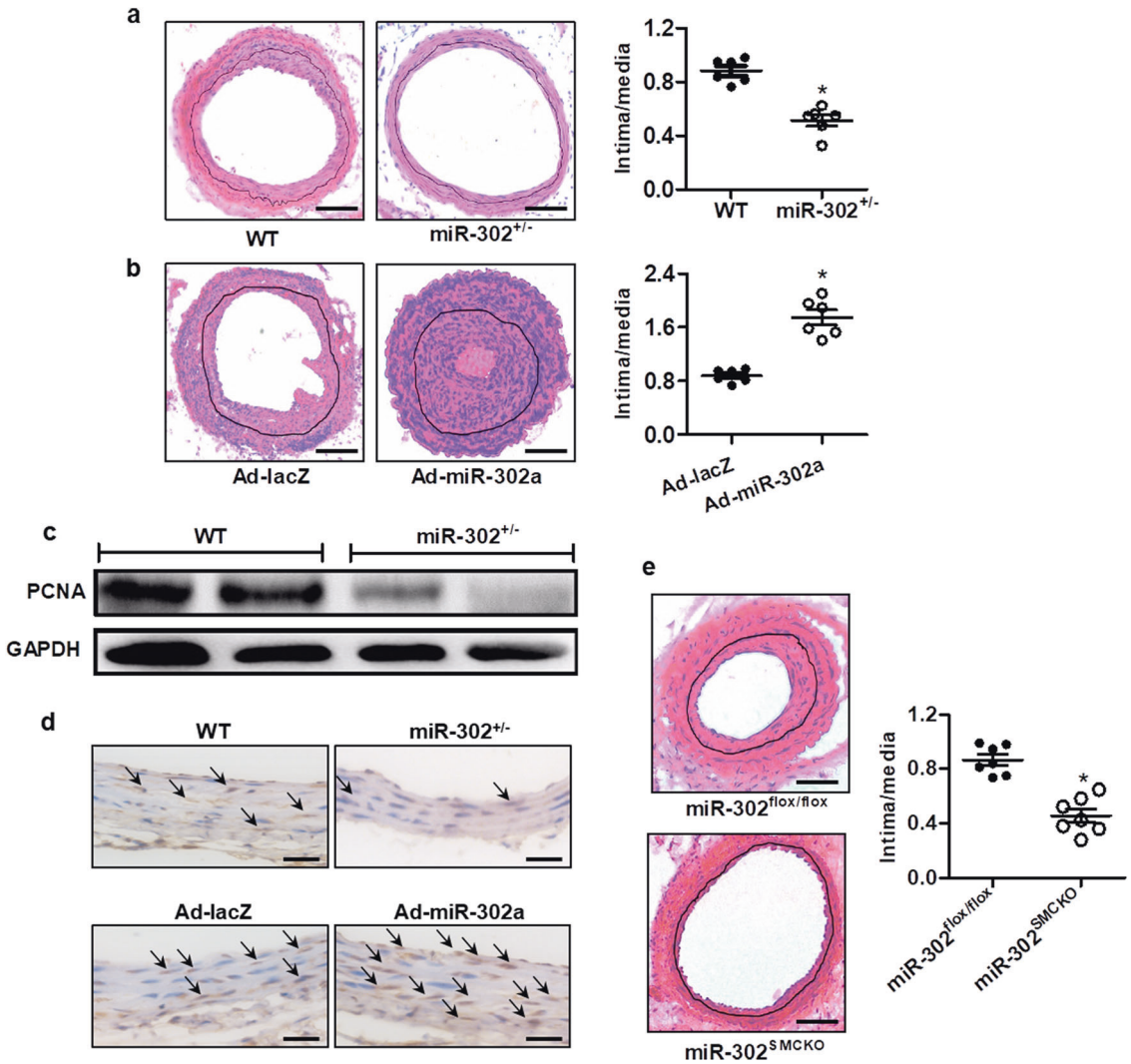

Fig. 1 Lack of miR-302 inhibits neointimal formation induced by carotid artery injury. a, **b** Twenty-one days after carotid artery injury, HE staining was performed to observe the intima and media thickness of carotid arteries from wild-type (WT) mice or miR-302 heterozygous (miR-302$^{+/-}$) mice (**a**) or in mice infected with lacZ adenovirus (Ad-lacZ) or miR-302a adenovirus (Ad-miR-302a) (**b**). Scale bar, 50 μm. The ratio of intima thickness to media thickness (intimal/medial) was quantified. *$P < 0.05$ vs. WT or Ad-lacZ, $n = 6$/group. **c** PCNA expression in the carotid arteries from wild-type mice or miR-302$^{+/-}$ mice after carotid artery injury. $n = 6$/group. **d** Immunohistochemical staining of Ki67 in carotid arteries. The arrows indicate Ki67-positive cells. Scale bar, 20 μm. $n = 8$/group. **e** HE staining revealed that SMC-specific knockout of miR-302 (miR-302^{SMCKO}) ameliorated neointimal formation and decreased the ratio of intimal thickness to medial thickness. Scale bar, 50 μm. *$P < 0.05$ vs. miR-302$^{flox/flox}$, $n = 7$/group.

substrate for horseradish peroxidase. The incorporation was measured at 450 and 540 nm on a microplate reader (Bio-Tek).

Flow cytometry for cell cycle analysis

MASMCs were collected by trypsin digestion and centrifugation at 200 × *g* for 5 min at 4 °C. The pellets were washed with ice-cold PBS and fixed in 70% ethanol for 24 h. Samples were then stained with staining buffer (PBS containing 50 μg/mL propidium iodide, 10 μg/mL RNase A, 0.1% sodium citrate, and 0.1% Triton X-100). DNA content was analyzed by flow cytometry (EPICS XL, Beckman Coulter, Miami, FL) to determine the fraction of cells in each phase of the cell cycle.

In vitro migration assay using scratch assay and Transwell chambers

MASMCs were cultured in 35-mm culture plates and then transfected with miR-302a mimics, miR-302a inhibitor, or the corresponding negative control. After 24 h, the cells were digested with trypsin and cultured in Culture-Insert 2 Well in μ-Dish 35 mm (IBIDI, Martinsried, Germany) in the presence of PDGF-BB for 24 h. The wound widths were measured using ImageJ software. Cell migration is presented as a percentage of the initial wound distance. For the Transwell assay, after the above treatment, cells were cultured in the upper chamber of the Transwell Assay Component (Corning Incorporated, Corning, NY) with 0.5% FBS. The lower chamber contained medium with 10% FBS. Forty-eight hours later, the cells in the lower chamber were fixed with 4% paraformaldehyde and stained with crystal violet. The images were obtained with a light microscope and quantified using ImageJ software.

Akt kinase activity assay

Cell lysates were subjected to immunoprecipitation using Akt antibody and protein G PLUS-Agarose (sc-2002, Santa Cruz Biotechnology, Santa Cruz, CA). The immunoprecipitated Akt was used to evaluate Akt kinase activity using a K-Lisa Akt activity kit (Millipore) according to the manufacturer's instructions. The

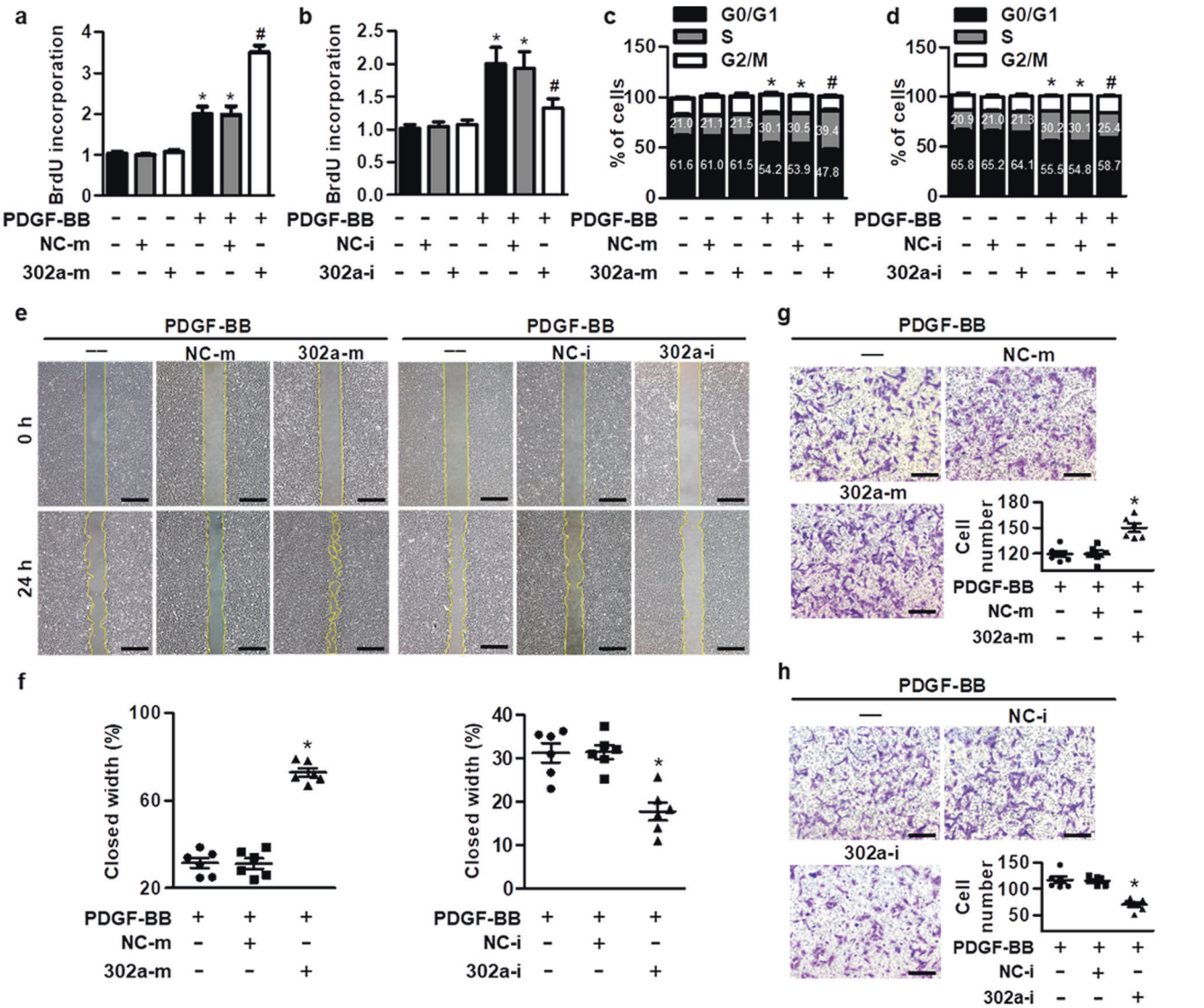

Fig. 2 MiR-302a potentiates PDGF-BB-induced MASMC proliferation and migration. a, **b** MASMCs were transfected with miR-302a mimics (302a-m, 50 nmol/L), mimics negative control (NC-m) (50 nmol/L) (**a**), miR-302a inhibitor (302a-i) (50 nmol/L), or inhibitor negative control (NC-i) (50 nmol/L) (**b**) for 24 h followed by PDGF-BB (20 ng/mL) treatment for 24 h. Cell proliferation was assessed by BrdU incorporation. **c**, **d** The percentages of cells in the G0/G1, S and G2/M phases of the cell cycle were analyzed. $^{*}P < 0.05$ vs. control, $^{\#}P < 0.05$ vs. PDGF-BB, $n = 8$. **e** Representative images of the scratch assay. Scale bar, 200 μm. **f** The quantification results for the wound closure assay. **g**, **h** Transwell analysis was performed. Representative images are shown. Scale bar, 100 μm. $^{*}P < 0.05$ vs. PDGF-BB, $n = 6$.

kinase activity was normalized to the Akt level in the immunoprecipitates determined by Western blotting.

PHLPP2 activity

Cell lysates were incubated with PHLPP2 antibody and protein G PLUS-Agarose overnight at 4 °C. Thereafter, the PHLPP2 immunoprecipitates were incubated with 5 mmol/L phosphatase substrate para-nitrophenyl phosphate (pNPP) in PBS at 30 °C. The absorbance was read at 405 nm using a microplate reader (Bio-Tek). The concentration of the product p-nitrophenol (pNP), which reflects the PHLPP2 activity, was determined by establishing a calibration curve from the plotted absorbance values corresponding to known concentrations of pNP. PHLPP2 activity was normalized to the protein content of immunoprecipitates.

Luciferase reporter assays

The full-length 3′UTR of mouse PHLPP2 was cloned into the psiCHECK-2 luciferase reporter vector (Promega,Madison, WI) at the *Xho*I and *Not*I sites. Mutants of the PHLPP2 3′UTR were constructed from the wild-type PHLPP2 3′UTR by site-directed mutagenesis. HEK293 cells were transfected with miR-302a mimics or mimics negative control and a luciferase reporter vector containing the wild-type or mutant 3′UTR of PHLPP2 using Hiperfect transfection reagent. Forty-eight hours later, firefly and Renilla luciferase activities were measured using the Dual-Glo Luciferase Assay System (Promega) and a microplate reader (TECAN Group Ltd, Mannedorf, Switzerland). The Renilla luciferase activity was normalized to the firefly luciferase activity.

Statistical analysis

All data are represented as the mean ± standard error. Statistical significance was tested by Student's *t*-test or one-way analysis of variance, followed by Duncan's multiple range tests. Statistical analysis was performed by SPSS 18.0 software (SPSS Inc., Chicago, IL). $P < 0.05$ was considered statistically significant.

RESULTS

Inhibition of miR-302 represses neointimal formation after carotid artery injury

Given the embryonic lethality in miR-302 homozygous mice [10], we generated adult miR-302 heterozygous mice and established a carotid artery injury model to investigate the role of miR-302 inneointimal formation (Fig. S1a–c). Carotid arteries were harvested following balloon angioplasty, and the intimal thickness to medial thickness ratio was measured. HE staining showed that neointimal formation gradually increased over the 21 days after injury (Fig. S1d). On day 21, knockdown of miR-302 significantly decreased intimal hyperplasia compared with that in wild-type mice, as demonstrated by the decreased ratio of intimal thickness to medial thickness (Fig. 1a). In contrast, upregulation of miR-302a by delivery of Ad-miR-302a in the carotid artery markedly increased the neointimal thickness compared with the Ad-lacZ control (Fig. 1b). Additionally, the expression levels of the cell proliferation markers PCNA and Ki67 were higher in carotid arteries from wild-type mice than in those from miR-302$^{+/-}$ mice. However, upregulation of miR-302a increased Ki67 levels in the carotid artery compared with that in the negative control group (Fig. 1c, d), indicating that miR-302a promotes neointimal formation and may be associated with VSMC hyperplasia. To support this notion, we further generated SMC-specific miR-302 knockout mice (Fig. S2a–c). Similar to the results in miR-302$^{+/-}$ mice, miR-302 deficiency in SMCs markedly attenuated carotid artery injury-induced increases in neointimal thickness (Fig. 1e).

Overexpression of miR-302 promotes MASMC proliferation and migration

To determine whether the effects of miR-302 on neointimal formation were due to the regulation of VSMC proliferation, MASMC growth and motility were examined. CCK-8 assay and BrdU incorporation showed that miR-302a overexpression enhanced PDGF-BB-induced cell viability and proliferation (Fig. 2a and Fig. S3a, b). Similar results were observed after serum stimulation (Fig. S3c, d). However, miR-302a knockdown inhibited PDGF-BB- or serum-induced increases in cell viability (Fig. 2b and Fig. S3e–h). Flow cytometric cell cycle analysis revealed that PDGF-BB-induced cell cycle progression was significantly accelerated by miR-302a overexpression. In miR-302a mimics-treated MASMCs after PDGF-BB treatment, 47.8%, 39.4%, and 13.9% of the cell population was in G_0/G_1 phase, S phase, and G_2/M phase, respectively, compared with 54.2%, 30.1%, and 15.5% of control cells, indicating that miR-302a enhances cell entrance into S phase

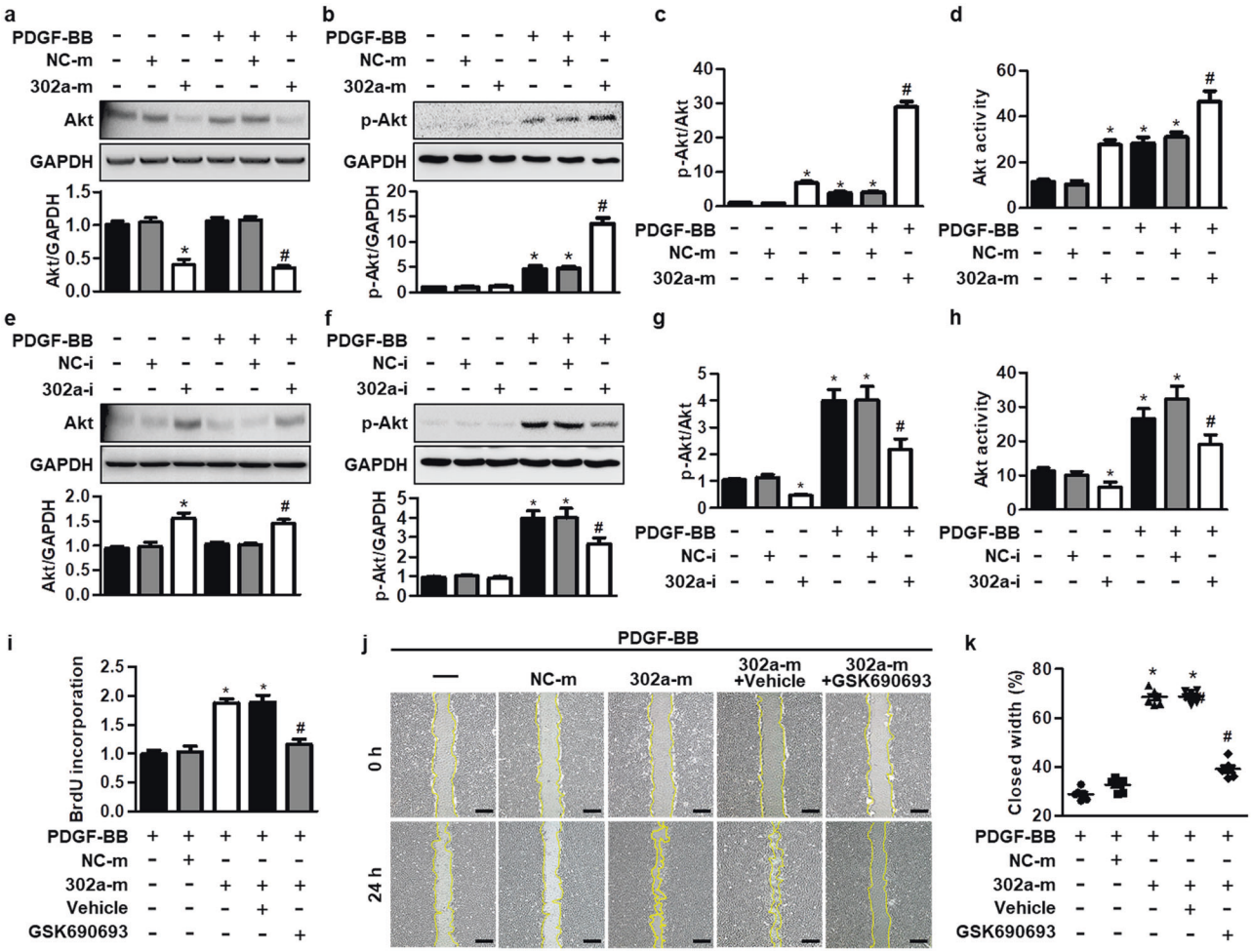

Fig. 3 MiR-302a regulates MASMC proliferation dependent on Akt signaling. a–d MASMCs were transfected with miR-302a mimics or mimics negative control for 24 h and then treated with recombinant PDGF-BB for another 1 h. The level of Akt (**a**) and p-Akt (**b**), the ratio of p-Akt to Akt (**c**), and Akt activity (**d**) were measured. **e–h** Akt (**e**) and p-Akt (**f**) levels, p-Akt/Akt ratio (**g**), and Akt activity (**h**) in cells transfected with miR-302a inhibitor or inhibitor negative control for 24 h followed by PDGF-BB treatment for 1 h. $^{*}P < 0.05$ vs. control, $^{\#}P < 0.05$ vs. PDGF-BB, $n = 6$. **i** After transfection with miR-302a mimics for 24 h, the cells were treated with GSK690693 (5 μmol/L) or 0.1% DMSO (vehicle) for another 24 h in the presence of PDGF-BB. Cell proliferation was examined by BrdU incorporation. **j** Representative images ofthe scratch assay. Scale bar, 200 μm. **k** The quantification results for the wound closure assay. $^{*}P < 0.05$ vs. PDGF-BB, $^{\#}P < 0.05$ vs. PDGF-BB + 302a-m, $n = 7$.

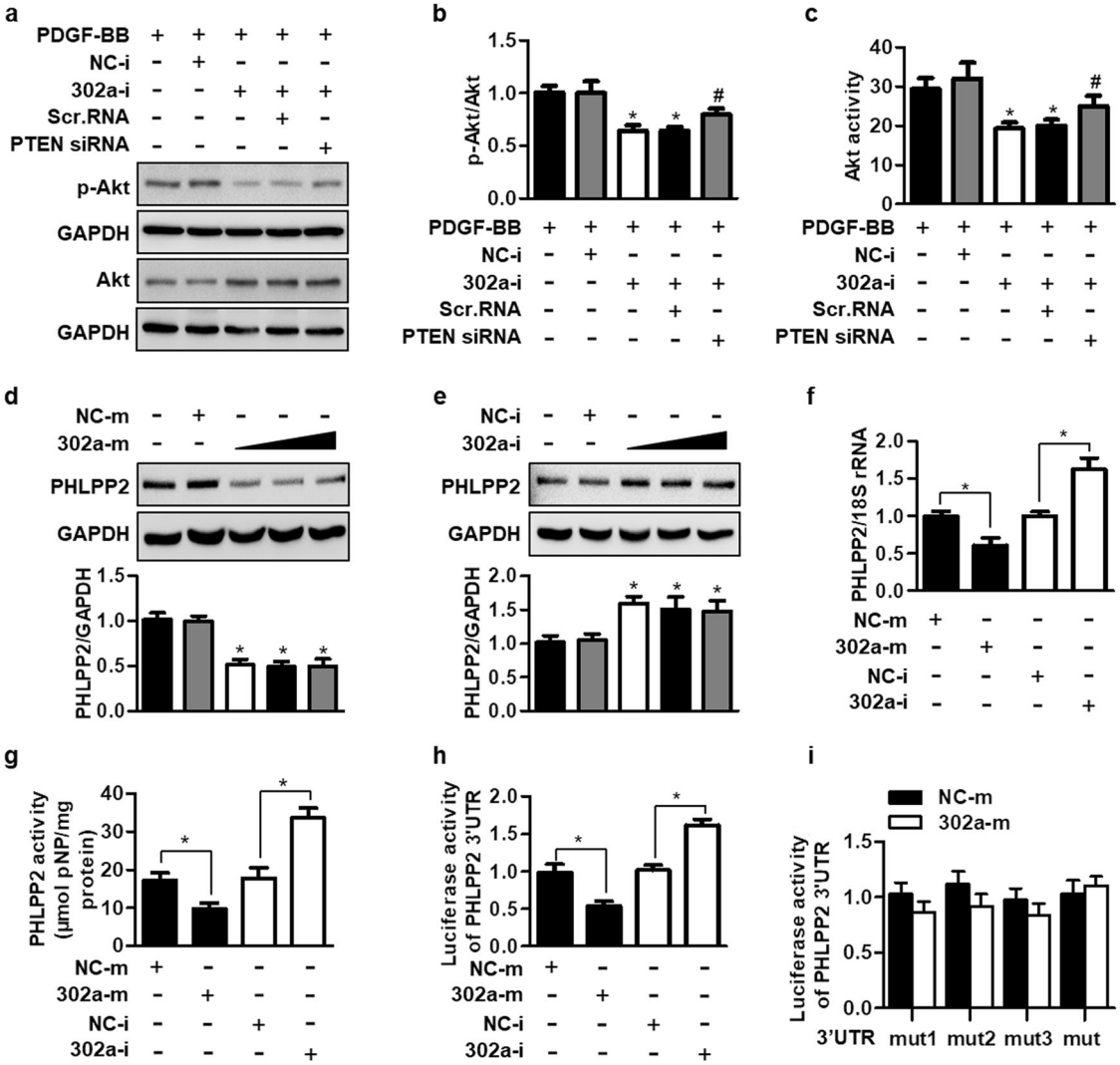

Fig. 4 MiR-302a targets PHLPP2 and negatively regulates its expression. a–c MASMCs were cotransfected with miR-302a inhibitor and PTEN siRNA (siPTEN) or scramble RNA (scr. RNA) for 24 h prior to PDGF-BB treatment for 1 h. Representative Western blotting images for p-Akt and Aktare shown (**a**). The ratio of p-Akt to Akt (**b**) and Akt activity (**c**) were determined. $^{*}P < 0.05$ vs. PDGF-BB, $^{\#}P < 0.05$ vs. PDGF-BB + 302-i, $n = 5$. **d**, **e** The protein expression of PHLPP2 in MASMCs transfected with different concentrations of miR-302a mimics (10, 20 and 50 nmol/L) (**d**) or miR-302a inhibitor (10, 20, and 50 nmol/L) (**e**). $^{*}P < 0.05$ vs. control, $n = 6$. **f**, **g** PHLPP2 mRNA level (**f**) and activity (**g**) in MASMCs transfected with miR-302a mimics or miR-302a inhibitor. **h**, **i** Luciferase reporter constructs containing wild-type PHLPP2 3′UTR (**h**) or PHLPP2 3′UTR mutations as indicated (**i**) were cotransfected along with miR-302a mimics or inhibitor in HEK293 cells for the luciferase activity assay. $^{*}P < 0.05$ vs. NC-m or NC-i, $n = 6$.

(Fig. 2c). In contrast, inhibition of miR-302a markedly suppressed cell cycle progression (Fig. 2d). To understand the molecular mechanism by which miR-302a enhances cell cycle progression, we analyzed the expression of the cell cycle-related proteins cyclin E1, CDK2, p21, and p27 in MASMCs. Overexpressing miR-302a enhanced the PDGF-BB-induced increase in cyclin E1 and CDK2 expression but suppressed p21 and p27 expression (Fig. S4a–d). MiR-302a inhibition showed the opposite results (Fig. S4e–h). Additionally, transfection of miR-302a mimics significantly potentiated the migratory capacity of MASMCs, whereas inhibition of miR-302a retarded wound closure, which lowered cell motility (Fig. 2e, f). The Transwell assay, an alternative assay for determining cell movement, revealed that overexpression of miR-302a increased the migratory ability of MASMCs (Fig. 2g). In contrast, miR-302a knockdown was associated with inhibited cell migration (Fig. 2h). We next examined the effect of miR-302a on matrix metalloproteinases (MMPs), a group of proteases that cleaves extracellular matrix structural proteins and subsequently regulates the migratory activity of SMCs [18]. PDGF-BB significantly increased MMP2 and MMP9 expression, and this increase was further enhanced by miR-302a overexpression but inhibited by miR-302a downregulation (Fig. S5a–d).

MiR-302a potentiates MASMC proliferation by increasing Akt activity

Considering the possible role of miR-302 in Akt signaling activation and the capacity of Akt to regulate cell growth [11–15], we explored the possibility that miR-302a promotes VSMC proliferation by regulating Akt activation. Consistent with previous studies [11, 13], Western blotting showed that upregulation of miR-302a significantly decreased Akt expression in MASMCs in the absence or presence of PDGF-BB (Fig. 3a). In contrast, PDGF-BB-induced phosphorylation of Akt was markedly potentiated by the miR-302a mimics (Fig. 3b). The ratio of p-Akt/Akt, which reflects Akt activation, was increased in miR-302a mimics-treated cells (Fig. 3c). This was further supported by the kinase assay in which miR-302a overexpression increased Akt

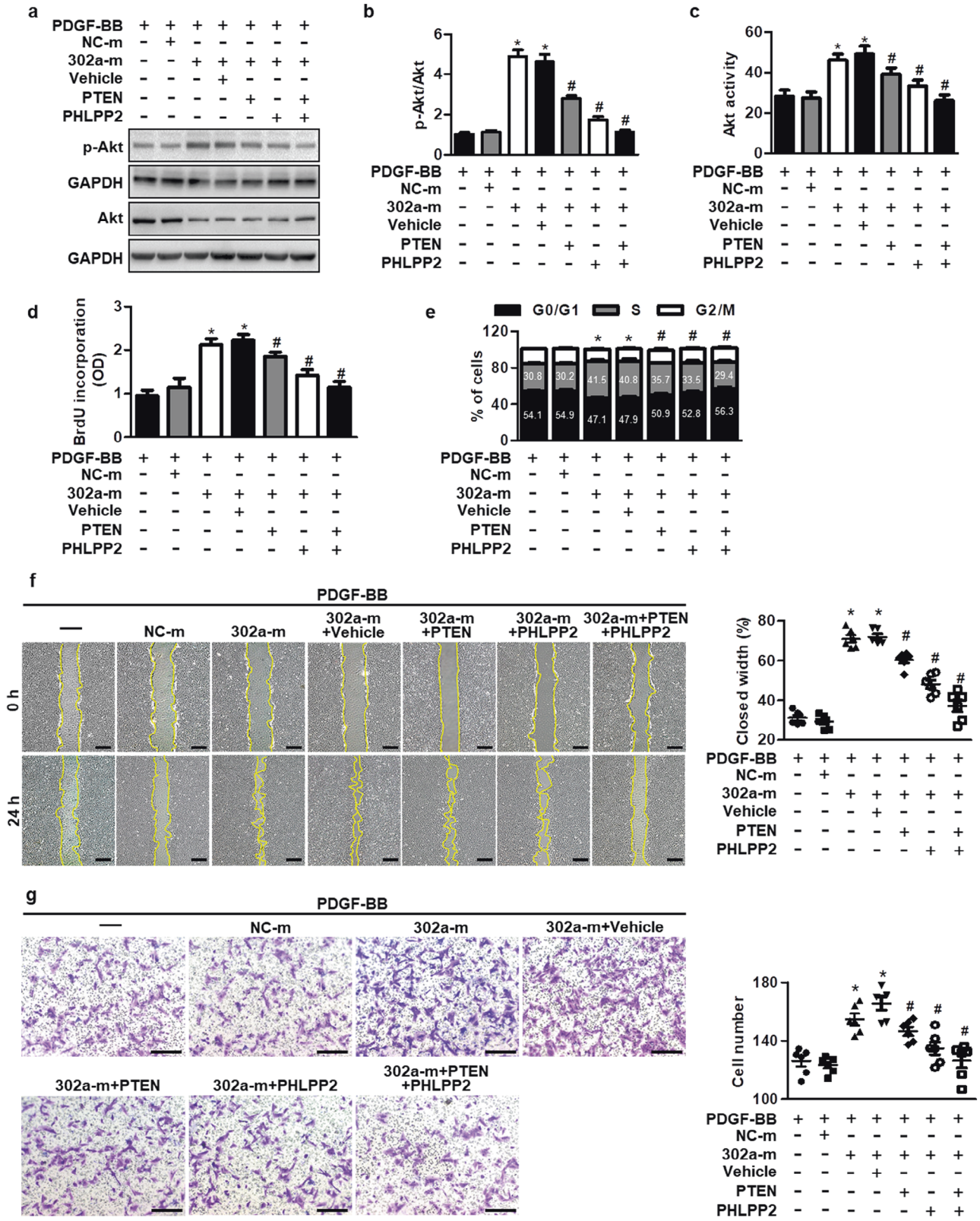

Fig. 5 Restoration of PHLPP2 or PTEN expression attenuates the effects of miR-302a on Akt activation, MASMC proliferation, and migration. a–**c** The cells were cotransfected with miR-302a mimics and pCMV vector (vehicle), PTEN plasmid, or PHLPP2 plasmid for 24 h and then treated with PDGF-BB for another 1 h. Representative Western blotting images for p-Akt and Akt are shown (**a**). The ratio of p-Akt to Akt (**b**) and Akt activity (**c**) were measured. **d**, **e** Cell viability (**d**) and cell cycle (**e**) analyses after PDGF-BB treatment for 24 h. **f**, **g** Cell migratory capacity was examined by the scratch assay (**f**) and Transwell analysis (**g**). Scale bar, 200 μm for the scratch assay and 100 μm for the Transwell analysis. $^{*}P < 0.05$ vs. PDGF-BB, $^{\#}P < 0.05$ vs. PDGF-BB + 302a-m, $n = 6$.

activity (Fig. 3d). Moreover, inhibition of miR-302a increased Akt expression, but attenuated PDGF-BB-induced the increase in Akt phosphorylation and activity (Fig. 3e–h). To further confirm whether Akt activity is required for the regulatory function of miR-302a in VSMC proliferation, cells were treated with miR-302a mimics and the Akt inhibitor GSK690693 in the presence of PDGF-BB. Compared with miR-302a mimics-treated MASMCs, treatment with GSK690693 inhibited cell proliferation and migration, which was potentiated by miR-302a upregulation (Fig. 3i–k). These results suggest that miR-302a regulates VSMC proliferation dependent on Akt signaling.

MiR-302a regulates the Akt signaling pathway at least by targeting PHLPP2

To investigate the mechanisms by which miR-302a regulates Akt activation, we initially tested the levels of p85 and p110, upstream of Akt. The results showed that neither miR-302a upregulation nor downregulation affected p85 or p110 levels (Fig. S6a–d). A previous study reported that miR-302a could target PTEN to activate Akt by increasing Akt phosphorylation [14]. Consistent with this study, miR-302a overexpression in MASMCs decreased PTEN expression, while suppression of miR-302a increased PTEN expression (Fig. S6e, f). However, it is worth noting that knockdown of PTEN only partially reversed the inhibitory effect of miR-302a knockdown on Akt phosphorylation and activity (Fig. 4a–c and Fig. S7), indicating that PTEN could not fully account for the effect of miR-302a on Akt activation. We identified three miR-302a seed target regions in the PHLPP2 mRNA 3′UTR using computational miRNA target prediction algorithms (Fig. S8). PHLPP2, a member of the PHLPP family, is a protein phosphatase that dephosphorylates Akt at the serine 473 residue to attenuate Akt signaling activation, thereby inhibiting cell proliferation [19, 20]. Western blotting and qPCR showed that PHLPP2 expression in MASMCs was inhibited by miR-302a overexpression but increased by miR-302a inhibition (Fig. 4d–f). PHLPP2 activity measurements revealed a similar tendency and indicated that miR-302a also reduced PHLPP2 activity (Fig. 4g). Furthermore, miR-302a upregulation decreased, whereas miR-302a downregulation elevated, the luciferase activity of the PHLPP2 3′UTR, as determined by the dual-luciferase reporter assay (Fig. 4h). Although miR-302a overexpression had no significant effects on the luciferase activity of PHLPP2 3′UTR mutants in which each single target site was mutated, the luciferase activity did not reach the level seen in the mimics negative control group. Nevertheless, when the three target sites were all mutated, the inhibitory effect of miR-302a on luciferase activity was completely abrogated, indicating that miR-302a targets PHLPP2 via three seed target regions (Fig. 4i).

Restoration of PHLPP2 expression inhibits the effects of miR-302a on Akt activation and MASMC motility

Next, we investigated whether the presence of PHLPP2 is required for miR-302a-mediated increase in MASMC proliferation by cotransfecting MASMCs with miR-302a mimics and a PHLPP2 expression plasmid. Overexpression of PHLPP2 or PTEN markedly attenuated the promoting effects of miR-302a on Akt phosphorylation and activity, and a combination of both exhibited a clear synergistic effect (Fig. 5a–c, and Fig. S9a, b). Moreover, the miR-302a-mediated enhancement of cell viability and cell cycle progression were inhibited by transfection with the PHLPP2 or PTEN plasmid. Similarly, stronger inhibitory effects were observed in the combination group (Fig. 5d, e). Additionally, the miR-302a-dependent promotion of cell motility was also partially attenuated in PHLPP2- or PTEN-overexpressing cells, whereas the combination of both completely offset the effects of miR-302a (Fig. 5f, g). Importantly, the inhibitory effects of overexpressing PHLPP2 on Akt activation and subsequent MASMC proliferation and motility were more pronounced than those of overexpressing PTEN, indicating that PHLPP2 may be more indispensable than PTEN for miR-302a function in MASMCs.

PHLPP2 is essential for the function of miR-302 in neointimal formation

To further evaluate the requirement of PHLPP2 during miR-302-regulated restenosis in vivo, Ad-shPHLPP2 was administered to miR-$302^{+/-}$ mice. As expected, increased expression of PHLPP2 was observed in carotid arteries from miR-$302^{+/-}$ mice compared with those from wild-type mice. The inhibitory effect of Ad-shPHLPP2 was confirmed by the reduced expression of PHLPP2 (Fig. 6a). Importantly, Ad-shPHLPP2 infection largely abolished the inhibition of neointimal formation that was observed in miR-$302^{+/-}$ mice (Fig. 6b).

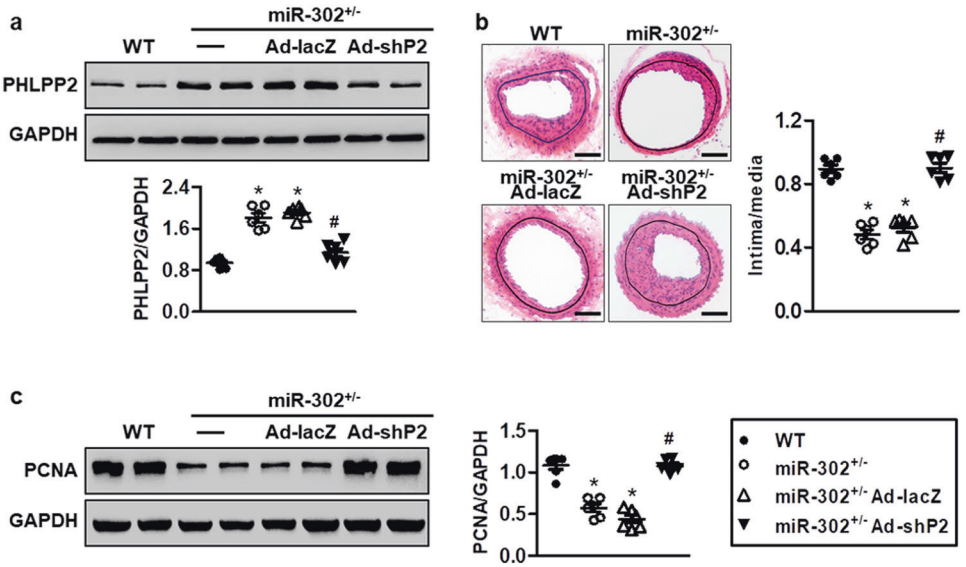

Fig. 6 MiR-302 knockdown ameliorates neointimal formation in a PHLPP2-dependent manner. a Wild-type mice and miR-$302^{+/-}$ mice were subjected to carotid artery injury. The PHLPP2 shRNA adenovirus (Ad-shP2) (1.0×10^{11} PFU) or Ad-lacZ (1.0×10^{11} PFU) was delivered to the injured arteries and incubated for 30 min. Twenty-one days after carotid artery injury, the carotid arteries were harvested for PHLPP2 protein expression determination. **b** HE staining was performed to observe the intima and media thickness of the carotid arteries of each group. Scale bar, 50 μm. The ratio of intima thickness to media thickness (intimal/medial) was quantified. **c** Western blotting analysis of PCNA expression in carotid arteries. $^{*}P < 0.05$ vs. WT, $^{\#}P < 0.05$ vs. miR-$302^{+/-}$, $n = 6$/group.

Moreover, the reduced PCNA expression in miR-302$^{+/-}$ mice was almost completely reversed by the knockdown of PHLPP2 (Fig. 6c). Therefore, the inhibitory effects of miR-302 knockdown on neointimal formation are largely dependent on the elevation of PHLPP2 expression.

DISCUSSION

To our knowledge, the present study is the first to show that miR-302a is involved in VSMC proliferation and vascular remodeling. The central findings of our work are summarized as follows. (1) Specific knockout of miR-302 in SMCs ameliorates neointimal formation. (2) miR-302a facilitates cell cycle progression and enhances VSMC proliferation and migration. (3) miR-302a decreases Akt protein expression while increasing Akt phosphorylation, leading to Akt activation. (4) miR-302a directly targets the 3′UTR of PHLPP2 and negatively regulates its expression.

It has been suggested that approximately 30%~60% of the protein-coding genes in humans are regulated by microRNAs [9, 21], indicating that miRNAs are widely involved in biological processes. Importantly, recent studies have shown that miRNAs are involved in regulating SMC proliferation and migration. For example, miR-9 targets PDGF receptor (PDGFR) and decreases its expression, leading to impairment of PDGF-PDGFR axis activation and subsequent SMC proliferation [22]. Moreover, miR-16 attenuates SMC proliferation and migration by inhibiting MAPK signaling through directly targeting of the cyclin D1 3′UTR [23]. In addition, miR-17/20 promotes pulmonary arterial SMC proliferation by regulating PHD2/HIF1 [24]. These findings indicate that miRNAs may be key therapeutic targets for the treatment of restenosis. Previous studies have implied that miR-302 could be a cancer therapeutic target due to its key role in regulating cancer cell proliferation and death [13, 21, 25]. Importantly, recent studies have also indicated the potential role of miR-302 in cardiac functions, such as cardiomyocyte proliferation, differentiation and death, and heart hypertrophy [26–29]. However, little is known about the regulatory role of miR-302 in vascular cell proliferation. In this study, we demonstrated that global knockdown or SMC-specific knockout of miR-302 ameliorated neointimal formation by inhibiting VSMC hyperplasia. The results were supported by the in vitro experiments, showing that miR-302a overexpression enhanced MASMC proliferation and migration, while inhibition of miR-302a was associated with inhibited MASMC proliferation and migration.

Akt signaling activation plays an important role in regulating cell growth, proliferation, migration, and survival [15]. Lack of Akt has been shown to inhibit VSMC proliferation and migration [15, 30]. Although miR-302 is involved in the regulation of Akt expression or activation [11–14], the precise function of miR-302a remains unclear and even controversial. Previous studies have shown that Akt is a potential target of miR-302, which is the mechanism underlying the inhibitory effect of miR-302 on cancer cell proliferation [11–13]. However, Li et al. showed that miR-302 activated Akt signaling by targeting PTEN in neuronal cells [14]. Presumably, this inconsistency may be due to the different roles of miR-302a in different cell types. Interestingly, in this study we demonstrated that miR-302a not only inhibited Akt protein expression but also potentiated Akt phosphorylation in VSMCs, resulting in Akt activation. These findings indicate that the effects of miR-302a on VSMC proliferation may be associated with increased Akt activation. Indeed, we further found that pharmacological inhibition of Akt almost completely reversed the promoting effects of miR-302a on VSMC proliferation and migration.

Mechanistically, our results showed that miR-302a decreased PTEN expression in MASMCs, which was consistent with a previous study [14]. Notably, in addition to the suppression of PTEN, we found that the promoting effect of miR-302a on Akt activation may be also mediated by targeting PHLPP2. PHLPP2 is a protein phosphatase that specifically dephosphorylates Akt at the serine 473 residue and blocks Akt downstream signaling [19]. Considering the known oncogenic role of Akt, pharmacologic PHLPP2 activators have thus been the subject of considerable research due to the therapeutic potential of PHLPP2 in neoplastic diseases [20, 31]. Until now, a few miRNAs have been identified to target PHLPP2, such as miR-25 and miR-493, leading to a suppression of cell proliferation [32, 33], indicating that these miRNAs are key regulators of PHLPP2 that can regulate Akt-dependent proliferation. Here, we demonstrated for the first time that PHLPP2 is a novel target of miR-302a, as demonstrated by the luciferase reporter assay. MiR-302a decreased PHLPP2 expression by binding to its 3′UTR, whereas inhibition of miR-302a was associated with increased PHLPP2 expression. More importantly, functional rescue experiments further suggested that PHLPP2 is a more crucial target that required for the miR-302a-mediated VSMC proliferation than PTEN, a well-known negative regulator of Akt.

In conclusion, we demonstrated that miR-302a potentiates VSMC hyperplasia and subsequent neointimal formation by Akt activation via targeting its phosphatase PHLPP2, suggesting that inhibition of miR-302a may be a novel strategy for restenosis treatment.

ACKNOWLEDGEMENTS

This work was supported by the National Natural Science Foundation of China (81525025, 81930106, 91739104, 81773723 and 81603098), National Key R&D Program of China (2017YFC0909302), Science and Technology Program of Guangzhou (201707010023), Fundamental Research Funds for the Central Universities (17ykjc29 and 17ykpy05), and High-level Health Teams of Zhuhai (2018).

AUTHOR CONTRIBUTIONS

JGZ and SJL designed the research; YYL performedthe research; YYL and XL analyzed the data; SJL wrote the paper.

ADDITIONAL INFORMATION

The online version of this article (https://doi.org/10.1038/s41401-020-0440-4) contains supplementary material, which is available to authorized users.

Competing interests: The authors declare no competing interests.

REFERENCES

1. Alexander MR, Owens GK. Epigenetic control of smooth muscle cell differentiation and phenotypic switching in vascular development and disease. Annu Rev Physiol. 2012;74:13–40.
2. Head SJ, Milojevic M, Daemen J, Ahn JM, Boersma E, Christiansen EH, et al. Mortality after coronary artery bypass grafting versus percutaneous coronary intervention with stenting for coronary artery disease: a pooled analysis of individual patient data. Lancet. 2018;391:939–48.
3. Fattori R, Piva T. Drug-eluting stents in vascular intervention. Lancet. 2003;361:247–9.
4. Xu K, Al-Ani MK, Pan X, Chi Q, Dong N, Qiu X. Plant-derived products for treatment of vascular intima hyperplasia selectively inhibit vascular smooth muscle cell functions. Evid Based Complement Altern Med. 2018;2018:3549312.
5. Lv XF, Zhang YJ, Liu X, Zheng HQ, Liu CZ, Zeng XL, et al. TMEM16A ameliorates vascular remodeling by suppressing autophagy via inhibiting Bcl-2–p62 complex formation. Theranostics. 2020;10:3980–93.
6. Huang Y, Shen XJ, Zou Q, Wang SP, Tang SM, Zhang GZ. Biological functions of microRNAs: a review. J Physiol Biochem. 2011;67:129–39.
7. Liu XY, Zhang FR, Shang JY, Liu YY, Lv XF, Yuan JN, et al. Renal inhibition of miR-181a ameliorates 5-fluorouracil-induced mesangial cell apoptosis and nephrotoxicity. Cell Death Dis. 2018;9:610.
8. Barroso-delJesus A, Romero-Lopez C, Lucena-Aguilar G, Melen GJ, Sanchez L, Ligero G, et al. Embryonic stem cell-specific miR302-367 cluster: human gene structure and functional characterization of its core promoter. Mol Cell Biol. 2008;28:6609–19.
9. Barroso-del Jesus A, Lucena-Aguilar G, Menendez P. The miR-302-367 cluster as a potential stemness regulator in ESCs. Cell Cycle. 2009;8:394–8.
10. Parchem RJ, Moore N, Fish JL, Parchem JG, Braga TT, Shenoy A, et al. MiR-302 is required for timing of neural differentiation, neural tube closure, and embryonic viability. Cell Rep. 2015;12:760–73.

11. Li X, Liu LL, Yao JL, Wang K, Ai H. Human umbilical cord mesenchymal stem cell-derived extracellular vesicles inhibit endometrial cancer cell proliferation and migration through delivery of exogenous miR-302a. Stem Cells Int. 2019;2019:8108576.
12. Ma YS, Lv ZW, Yu F, Chang ZY, Cong XL, Zhong XM, et al. MicroRNA-302a/d inhibits the self-renewal capability and cell cycle entry of liver cancer stem cells by targeting the E2F7/AKT axis. J Exp Clin Cancer Res. 2018;37:252.
13. Zhang GM, Bao CY, Wan FN, Cao DL, Qin XJ, Zhang HL, et al. MicroRNA-302a suppresses tumor cell proliferation by inhibiting AKT in prostate cancer. PLoS ONE. 2015;10:e0124410.
14. Li HH, Lin SL, Huang CN, Lu FJ, Chiu PY, Huang WN, et al. miR-302 attenuates amyloid-beta-induced neurotoxicity through activation of Akt signaling. J Alzheimers Dis. 2016;50:1083–98.
15. Stabile E, Zhou YF, Saji M, Castagna M, Shou M, Kinnaird TD, et al. Akt controls vascular smooth muscle cell proliferation in vitro and in vivo by delaying G_1/S exit. Circ Res. 2003;93:1059–65.
16. Liang SJ, Zeng DY, Mai XY, Shang JY, Wu QQ, Yuan JN, et al. Inhibition of Orai1 store-operated calcium channel prevents foam cell formation and atherosclerosis. Arterioscler Thromb Vasc Biol. 2016;36:618–28.
17. Guo JW, Liu X, Zhang TT, Lin XC, Hong Y, Yu J, et al. Hepatocyte TMEM16A deletion retards NAFLD progression by ameliorating hepatic glucose metabolic disorder. Adv Sci. 2020;7:1903657.
18. Kessenbrock K, Plaks V, Werb Z. Matrix metalloproteinases: regulators of the tumor microenvironment. Cell. 2010;141:52–67.
19. Kim K, Qiang L, Hayden MS, Sparling DP, Purcell NH, Pajvani UB. mTORC1-independent Raptor prevents hepatic steatosis by stabilizing PHLPP2. Nat Commun. 2016;7:10255.
20. Newton AC, Trotman LC. Turning off AKT: PHLPP as a drug target. Annu Rev Pharmacol Toxicol. 2014;54:537–58.
21. Guo Y, Cui J, Ji Z, Cheng C, Zhang K, Zhang C, et al. miR-302/367/LATS2/YAP pathway is essential for prostate tumor-propagating cells and promotes the development of castration resistance. Oncogene. 2017;36:6336–47.
22. Ham O, Lee SY, Song BW, Lee CY, Lee J, Seo HH, et al. Small molecule-mediated induction of miR-9 suppressed vascular smooth muscle cell proliferation and neointima formation after balloon injury. Oncotarget. 2017;8:93360–72.
23. Wang DW, Wang YQ, Shu HS. MiR-16 inhibits pituitary adenoma cell proliferation via the suppression of ERK/MAPK signal pathway. Eur Rev Med Pharmacol Sci. 2018;22:1241–8.
24. Chen T, Zhou Q, Tang H, Bozkanat M, Yuan JX, Raj JU, et al. miR-17/20 Controls Prolyl hydroxylase 2 (PHD2)/hypoxia-inducible factor 1 (HIF1) to regulate pulmonary artery smooth muscle cell proliferation. J Am Heart Assoc. 2016;5:e004510.
25. Liang Z, Bian X, Shim H. Inhibition of breast cancer metastasis with microRNA-302a by downregulation of CXCR4 expression. Breast Cancer Res Treat. 2014;146:535–42.
26. Kuppusamy KT, Sperber H, Ruohola-Baker H. MicroRNA regulation and role in stem cell maintenance, cardiac differentiation and hypertrophy. Curr Mol Med. 2013;13:757–64.
27. Fang YC, Yeh CH. Inhibition of miR-302 suppresses hypoxia-reoxygenation-induced H9c2 cardiomyocyte death by regulating Mcl-1 expression. Oxid Med Cell Longev. 2017;2017:7968905.
28. Li G, Song Y, Li YD, Jie LJ, Wu WY, Li JZ, et al. Circulating miRNA-302 family members as potential biomarkers for the diagnosis of acute heart failure. Biomark Med. 2018;12:871–80.
29. Xu F, Yang J, Shang J, Lan F, Li M, Shi L, et al. MicroRNA-302d promotes the proliferation of human pluripotent stem cell-derived cardiomyocytes by inhibiting LATS2 in the Hippo pathway. Clin Sci. 2019;133:1387–99.
30. Shi L, Ji Y, Jiang X, Zhou L, Xu Y, Li Y, et al. Liraglutide attenuates high glucose-induced abnormal cell migration, proliferation, and apoptosis of vascular smooth muscle cells by activating the GLP-1 receptor, and inhibiting ERK1/2 and PI3K/Akt signaling pathways. Cardiovasc Diabetol. 2015;14:18.
31. Gao MH, Miyanohara A, Feramisco JR, Tang T. Activation of PH-domain leucine-rich protein phosphatase 2 (PHLPP2) by agonist stimulation in cardiac myocytes expressing adenylyl cyclase type 6. Biochem Biophys Res Commun. 2009;384:193–8.
32. Zhang J, Bai R, Li M, Ye H, Wu C, Wang C, et al. Excessive miR-25-3p maturation via N(6)-methyladenosine stimulated by cigarette smoke promotes pancreatic cancer progression. Nat Commun. 2019;10:1858.
33. Deng J, Ma M, Jiang W, Zhang H, Cui S. MiR-493 promotes prostate cancer cells proliferation by targeting PHLPP2 and activating Akt signaling pathway. Clin Lab. 2019;65. https://doi.org/10.7754/Clin.Lab.2018.180806.